Isospin distribution of quadrupole strength in ^{118}Sn: Comparison with pion, nucleon, and electron scattering

V. R. Brown
Lawrence Livermore National Laboratory, University of California, Livermore, California 94550

J. A. Carr
Supercomputer Computations Research Institute, The Florida State University, Tallahassee, Florida 32306

V. A. Madsen
Physics Department, Oregon State University, Corvallis, Oregon 97331

F. Petrovich
Physics Department, Florida State University, Tallahassee, Florida 32306

(Received 6 November 1987)

The isospin structure of the quadrupole strength in ^{118}Sn is examined by a variety of means in an attempt to understand the surprisingly large amount of isovector strength extracted from some recent π^-/π^+ experiments in the excitation-energy region (below $2\hbar\omega$) expected for the isoscalar giant-quadrupole resonance. The ratio of the giant-quadrupole resonance neutron and proton multipole matrix elements for ^{118}Sn determined from π^-/π^+ data is $M_n/M_p = 1.9 \pm 0.4$ compared to calculations which range from 1.1 to about N/Z (1.36). It is demonstrated that this large ratio has unrealistic consequences in random-phase approximation mixing of the giant states into the first 2^+ state transition (core polarization), which has been independently studied by other probes and is in rather good agreement with quasiparticle random-phase approximation calculations, which have $M_n/M_p \leq N/Z$ for the isoscalar giant-quadrupole resonance. Quasiparticle random-phase approximation transition densities are used to calculate pion, proton, and neutron cross sections to the isoscalar giant-quadrupole resonance and the first 2^+ state using microscopic reaction models. A comparison of $B(E2)$ from the same structure model is made to the various data for the first 2^+ transition and to the ^{116}Sn(e,e') data on the isoscalar giant-quadrupole resonance. Although not completely conclusive because of the lack of reliable (e,e') data, the evidence from all these comparisons is that the π^-/π^+ results are at odds with the results of other probes and with nuclear structure theory and that the problem seems to be with the π^+ scattering results.

I. INTRODUCTION

Over the past ten years it has been well established[1-5] that there can be a measurable difference between the neutron and proton deformation parameters for the first 2^+ vibrational states of even nuclei. Although both types of nucleons participate in the vibration, a shell closure in neutrons (protons) inhibits the collective vibration of neutrons (protons). The type of nucleon involved in the shell closure will therefore tend to have a smaller vibrational deformation parameter than the other type. The multipole matrix elements,

$$M_{(n,p)} = \left\langle f \left| \left| \sum_{i=1}^{(N,Z)} r_i^\lambda Y_\lambda(\hat{\mathbf{r}}_i) \right| \right| i \right\rangle , \quad (1)$$

thus have ratios of M_n/M_p which may differ from the value N/Z for the collective model of a homogeneous nuclear fluid, and this deviation has been shown to be in the direction of the dominant shell effects. Differences between M_n and M_p are also, in principle, expected for the lowest 2^+ states in open-shell nuclei, but these are generally much smaller than for single-closed-shell (SCS) nuclei. It has been shown[5] that there is a sudden jump in the direction of equality between M_n/M_p and N/Z when only one pair of nucleons (or holes) is added to a magic number of nucleons.

Although these ratios for low-lying 2^+ states are very dependent on the details of the valence configurations, this should not be true of giant resonances since they are shell-breaking excitations. Schematic-model results[4] give $|M_n/M_p| \leq N/Z$ for the isoscalar and isovector giant resonances over a wide range of nuclei. The fact that M_n/M_p can be more isoscalar than the hydrodynamical model is consistent with the collective-model for the giant-quadrupole isoscalar resonance (GQR) of Bohr and Mottelson[6] and is a result of the stronger coupling of the protons to the neutron excess. It is true that the mixing of the low-lying 2^+ collective strength and the GQR is substantial, but we will show in this paper that it is the mixing of the GQR into the low-lying region (core polarization) that produces the main effect in transitions. Mixing of the low-lying strength into the GQR also occurs; however, because of the energy-weighted sum rule in the random-phase approximation (RPA), this upward mixing or "reverse" core polarization into the GQR is insignificant. Furthermore, it produces an effect in the transition matrix elements that is in the wrong direction

to explain some surprising recent pion-scattering results for neutron SCS nuclei such as ^{118}Sn.

The pion work in question[7] consists of experiments comparing π^+ and π^- inelastic excitation of giant resonances in ^{118}Sn. This work yields a surprisingly small ratio of $M_n/M_p=1.27\pm0.26$ for the first 2^+ state and a surprisingly large ratio of $M_n/M_p=1.9\pm0.4$ for the GQR. The Sn isotopes are neutron-valence nuclei, so it is expected that the 2_1^+ state should have a value of $M_n/M_p>N/Z$. This is, in fact, the case, with the mean ratio[2] from previously available data equal to 1.72 ± 0.21. As mentioned above and discussed further below, the GQR, on the other hand, is expected to be both more isoscalar than the 2_1^+ and little affected by the isospin composition of the 2_1^+ transition. However, the pion results for the GQR yield M_n/M_p not just greater than N/Z but greater *even* than the established 2_1^+ ratio. Another pion experiment[8] on ^{208}Pb has also reported a very large value of $M_n/M_p=3.8\pm1.2$ for the GQR. We will also make some mention of theoretical results for ^{208}Pb below.

The purpose of this paper is to discuss the ratios of M_n/M_p for the giant-quadrupole resonances determined from several points of view, starting with the schematic-model Tamm-Dancoff approximation (TDA) and RPA results and working up to full nondegenerate quasiparticle RPA calculations. We emphasize the connection between the M_n/M_p for the giant resonances and that already observed by a variety of probes for the 2_1^+ state transition. The quasiparticle RPA transition densities are used to calculate inelastic nucleon and pion scattering cross sections to the low-lying 2_1^+ state and pion scattering to the isoscalar GQR region in ^{118}Sn. Section II contains a discussion of giant resonances within the schematic model, including the effects of mixing between the high-lying and low-lying 2^+ states. Section III contains a discussion of a degenerate RPA model which does not use perturbation theory for the core polarization. This model illustrates the features of mixing of the dominant collective states. Section IV contains a study of the effects on M_n and M_p from using a more realistic nondegenerate RPA model. Section V presents the results of cross section calculations for inelastic pion, nucleon, and electron scattering based on the neutron and proton RPA transition densities described in Sec. IV. Section VI contains a discussion of these results including a comparison of our results with other calculations of giant resonances. Also included in Sec. VI is a calculation of the effects of core polarization on the 2_1^+ using M_n/M_p for the GQR as determined from π^-/π^+. Section VII contains our conclusions.

II. THE SCHEMATIC MODEL OF QUADRUPOLE GIANT RESONANCES

In our earlier work[1-5] on low-lying 2^+ states we used the schematic model[4] for giant resonances and then coupled these giant resonances via perturbation theory to the first 2^+ vibrational state. The core polarization on the 2_1^+ transition was then expressed in terms of either the matrix

$$\underset{\sim}{\varepsilon}=\begin{bmatrix}\varepsilon_{00} & \varepsilon_{01}\\ \varepsilon_{10} & \varepsilon_{11}\end{bmatrix} \tag{2a}$$

in the isospin representation or

$$\underset{\sim}{\delta}=\begin{bmatrix}\delta^{nn} & \delta^{np}\\ \delta^{pn} & \delta^{pp}\end{bmatrix} \tag{2b}$$

in the neutron-proton representation. The M_n/M_p obtained from these parameters are appropriate for the 2_1^+ transition and not the GQR transitions. The mixing of the giant resonance into the 2_1^+ state has a very large effect on the multipole matrix elements, increasing M_n by a factor of 2 or more and driving M_n/M_p from infinity (valence neutrons) towards N/Z.

The giant-resonance transition amplitude, an ingredient in the core-polarization parameters, is also available from the schematic model. Using Eq. (16) of Ref. 4 we may write, for giant-resonance t, the ratio

$$M_n/M_p=(S_0^t+S_1^t)/(S_0^t-S_1^t)\approx 1+\frac{(y_n-y_p)}{(y_n+y_p)}\left[\frac{\alpha+\beta}{\beta}\right], \tag{3}$$

where α and β are the like- and unlike-nucleon interaction strengths,[4] and

$$y_{(n,p)}=\sum_{mi}^{(N,Z)}|\langle mi\,|\,r^\lambda Y_\lambda(\hat{\mathbf{r}})\,|\,0\rangle^2| \tag{4}$$

are sums over individual particle-hole (p-h) transition strengths for neutrons or protons, which are calculated[4] using $2\hbar\omega$ harmonic-oscillator quadrupole sum rules. Using Eq. (33) of Ref. 4 with the assumptions that the neutron and proton rms radii are equal and that $\beta/\alpha=3$, the TDA result of Eq. (3) for ^{118}Sn is that $M_n/M_p=1.14$. For a realistic neutron skin[9] with the ratio of the neutron and proton rms radii $r_n/r_p=1.04$, it is 1.24. An RPA version of the same degenerate model of the giant resonances gives $M_n/M_p=1.27$ using $r_n/r_p=1.04$. All three of these results are lower than $N/Z=1.36$ and much lower than the reported[7] ratio of 1.9. The reason that the GQR ratio is between unity and N/Z is that the interaction couples the neutrons and protons to make the transition more isoscalar by lowering the neutron strength and raising the proton strength. This same effect was mentioned earlier in a collective-model context.

In the case of ^{118}Sn there is a large neutron excess, so one might wonder whether there should not be some valence space ($0\hbar\omega$) mixing into the giant resonances, i.e., "reverse" core polarization. In the RPA schematic-model perturbation treatment[10] of configuration mixing, the core polarization and "reverse" core polarization parameters are given by

$$\underset{\sim}{\delta}^{RPA}=\frac{2}{\hat{\lambda}^2}\sum_b\frac{E_b\underset{\sim}{\mathcal{M}}_b\underset{\sim}{\mathcal{M}}_b^T\underset{\sim}{V}}{(E_a)^2-(E_b)^2}, \tag{5a}$$

where λ is the multipolarity, $\underset{\sim}{\delta}$ is the 2×2 matrix given in Eq. (2b), $\underset{\sim}{\mathcal{M}}$ is a 2×1 matrix containing M_n and M_p,

$$\underset{\sim}{\mathcal{M}} = \begin{bmatrix} M_n \\ M_p \end{bmatrix} , \tag{5b}$$

and $\underset{\sim}{V}$ is a 2×2 matrix of separable multipole interaction strengths[4]

$$\underset{\sim}{V} = \begin{bmatrix} \alpha & \beta \\ \beta & \alpha \end{bmatrix} , \tag{5c}$$

with diagonal elements equal to like-particle and nondiagonal elements equal to the unlike-particle interaction strengths. The index a represents the state in the space being polarized, while b represents the states in the core space, and $\hat{\lambda} = (2\lambda+1)^{1/2}$.

The mixing of the high- and low-lying 2^+ excitations represented by Eq. (5a) is not symmetric. The most important difference arises from the fact that for "reverse" core polarization the energy in the numerator represents the $0\hbar\omega$ two-quasiparticle energies, which combine with the low-lying multipole matrix elements to give very little effect on the high-lying GQR because of the reduced energy weighting. In addition, the energy denominator involved in the mixing coefficient is equal in magnitude but opposite in sign to the usual core polarization. The sign is positive (constructive) for mixing of the high state into the low state but negative (destructive) for the mixing of the low state into the high state. Therefore, what mixing there is, in the case of a neutron-valence nucleus like Sn, lowers the giant-resonance neutron strength, making the ratio M_n/M_p even smaller than the results of the schematic models without "reverse" core polarization given above.

III. DEGENERATE RPA MODEL

A degenerate RPA model has been developed to illustrate how the quadrupole isospin strength is distributed by the mixing of the dominant collective states. The RPA equations with a separable particle-hole interaction can be written[10,11] in a matrix form as

$$\underset{\sim}{H}\underset{\sim}{F} = E^2\underset{\sim}{F} , \tag{6}$$

where E is the energy of the state in the presence of the interaction,

$$\underset{\sim}{H}^{\text{int}}_{ij} = \frac{2}{\hat{\lambda}^2}\xi_i^{1/2}\underset{\sim}{\mathcal{M}}_i^T\underset{\sim}{V}\underset{\sim}{\mathcal{M}}_j\xi_j^{1/2} , \tag{7}$$

and ξ is the unperturbed energy of the two-quasiparticle state i. In Eq. (7) $\underset{\sim}{\mathcal{M}}_j$ is now an $N\times 2$ matrix, which contains unperturbed single-particle matrix elements M_n and M_p of the state j, and $\underset{\sim}{V}$ is the 2×2 matrix of the interaction strength described in connection with Eq. (5). $\underset{\sim}{F}$ is an $N\times 1$ matrix of the RPA amplitude solutions. In the nondegenerate case the dimension N corresponds to the number of independent two-quasiparticle states which all occur at different energies.

If we apply Eqs. (6) and (7) to the degenerate model, the noncollective states in each space are devoid of multipole strength and are each uncoupled from all other states both inside and outside of their spaces. We are, therefore, able to work on a reduced eigenvalue problem which includes only the collective states in each space, $0\hbar\omega$, $2\hbar\omega$, etc., treated separately. The eigenvalue problem, when we consider coupling among these spaces, looks the same as given in Eqs. (6) and (7), except now the matrix to be diagonalized is simply dimensioned according to the number of collective states to be considered. The ξ are the energies of these unperturbed collective states, and $\underset{\sim}{\mathcal{M}}$ is the matrix of the collective multipole matrix elements. In the degenerate model the particle-hole energies are all taken as equal for the various spaces included in the calculation. Because of the degeneracy, the sum-rule strength for a given isospin and multipolarity is concentrated entirely in the collective states and not spread out over an extended energy range as is the case when nondegeneracy, two-particle two-hole, and continuum effects are considered.

For the neutron-valence SCS nucleus ^{118}Sn, the dominant quadrupole collective states could be taken as the lowest-lying collective state and the isoscalar and isovector giant states. The particle-hole structure of these states involves the $0\hbar\omega$ and $2\hbar\omega$ spaces. In a recent paper[12] we described another low-lying (somewhat collective) transition that involves $1\hbar\omega$ even-parity particle-hole partners, with the hole in the spin-orbit intruder level of the closed-shell-type nucleon. We have called these states "reversal states" because their isospin properties are opposite to those of the 2_1^+ transition. The systematic existence of such states is yet to be demonstrated empirically. Nevertheless, for illustrative purposes we include these states, making our degenerate RPA model calculation for ^{118}Sn a four-state diagonalization problem.

For our model problem, then, the unperturbed strength is made up of four types of excitations: valence neutrons, proton spin-orbit intruder p-h pairs,[12] an isoscalar giant resonance, and an isovector giant resonance. An RPA schematic model is applied to each space separately before diagonalizing. The effective interaction is determined by placing the giant-quadrupole isoscalar state at the empirical energy $64A^{-1/3}$ and the isovector state at an energy $113A^{-1/3}$, which for lack of empirical information is made consistent with the nondegenerate RPA calculation described in Sec. IV. In order to preserve the unlike-to-like particle-hole interaction-strength ratio of three-to-one, an effective mass ratio of 0.83 is used.[10] As discussed in Sec. II, a realistic neutron skin[9] is included in the calculation by taking a value of 1.04 for the ratio of the neutron and proton rms radii.

The unperturbed values of M_n and M_p and the starting energies are given in the input columns of Table I. Because the collective states have all the sum-rule strength concentrated at a given energy, the diagonalization in the four-state model tends to push the low-lying 2^+ states relatively lower in energy than in the nondegenerate quasiparticle RPA (QRPA). To compensate for this it is necessary to choose starting energies somewhat higher than the mean degenerate energy of the QRPA. Our procedure for adjusting the starting energies preserves the energy-weighted sum rule. The unperturbed proton reversal state is placed slightly above the appropriate p-h energy for the spin-orbit intruder and its partner $(\pi 4g_{\frac{9}{2}})^{-1}(\pi 4d_{\frac{5}{2}})$ at 5 MeV. The starting energy of the 2_1^+

TABLE I. Neutron and proton multipole matrix elements M_n and M_p in fm^2 in a degenerate RPA four-state model for ^{118}Sn. The four states are the isoscalar and isovector giant-quadrupole resonances, the reversal state, and the 2_1^+ state. The unperturbed and perturbed energies are in MeV. The input includes the energy-weighted harmonic-oscillator sum-rule strengths with an effective mass of 0.83. The $2\hbar\omega$ space has already been diagonalized. The output columns contain the results for the four transitions after the four-state diagonalization.

	Input				Output			
State	E	M_n	M_p	M_n/M_p	E	M_n	M_p	M_n/M_p
2_1^+	2.61	31.7	0.0	∞	1.23	82.1	46.3	1.77
Reversal	5.00	0.0	18.9	0.0	4.85	8.3	24.6	0.34
Isoscalar GQR	13.05	76.7	60.3	1.27	13.3	72.7	57.1	1.27
Isovector GQR	23.0	54.4	−48.2	−1.13	23.0	54.6	−48.4	−1.13

Empirical (GQR): $M_p = 63.0 \pm 13.0$[a] and $M_n/M_p = 1.9 \pm 0.4$ with $M_p = 31.0 \pm 1.3$[b]
Empirical (2_1^+): $M_p = 45.5 \pm 0.4$[c] and $M_n/M_p = 1.72 \pm 0.21$[d]
$= 1.27 \pm 0.25$[e]

[a]Based on sum-rule estimate for ^{116}Sn from Ref. 13 (arbitrary 20% error).
[b]See Ref. 7, where M_p has been determined assuming the proton sum-rule strength reported in Ref. 7 is concentrated at 13.2 MeV.
[c]$M_p = [B(E2)\uparrow]^{1/2}$ from Ref. 2.
[d]See Refs. 2 and 14.
[e]Calculated from data of Ref. 7 using formulas from Ref. 2.

state is obtained from a degenerate two-quasiparticle model with pairing and then adjusted upward to 2.61 MeV, resulting in the solution energy at the experimental position of 1.23 MeV.

The results after diagonalization are shown in the output columns of Table I. The energy-weighted sum rule is preserved but redistributed by the diagonalization as it is in the full nondegenerate quasiparticle RPA calculation described in Sec. IV. The results of the four-state diagonalization are quite consistent with the results of the more realistic nondegenerate calculation of Sec. IV. One can see from this simple model that the effect of mixing from the giant states (core polarization) on the 2_1^+ transition is substantial both in increasing the magnitude of M_n and M_p and in changing the ratio of M_n/M_p from pure neutron to a value just greater than $N/Z = 1.36$. After diagonalization both M_n/M_p and M_p are completely consistent with previous data.[2] The reversal state changes from pure proton to values of M_n/M_p and M_p consistent with the full nondegenerate RPA calculation.[12] This result has not been confirmed empirically.

The giant states have $|M_n/M_p| < N/Z$. The isoscalar GQR is of particular interest here in comparison to the π^-/π^+ scattering result[7] of 1.9 ± 0.4. The value of $M_n/M_p = 1.27$ for the isoscalar GQR is much lower than the π^-/π^+ result; it is also less than N/Z but greater than the value of 1.1 obtained in our full nondegenerate RPA calculations described in the next section. The reason for the difference is that in the full nondegenerate calculation the energy-weighted sum-rule strength is not fully concentrated at a single energy (13.3 MeV in this case), and certain $2\hbar\omega$ spin-orbit intruder states carry some strength above the resonance region.

IV. NONDEGENERATE RPA MODEL

So far we have been considering idealizations in which all particle-hole or two-quasiparticle states in a given space are degenerate. We now go to results of an open-shell RPA calculation with the unperturbed energies determined by the Nilsson parameters[15] and pairing. When nondegeneracy of the individual two quasiparticles is included, the giant-resonance strength, isolated in one isoscalar and one isovector state in the degenerate schematic model, gets spread out over many states. We have calculated M_n and M_p for all states arising from applying quasiparticle RPA to the spherical Nilsson model configurations from $2d\frac{5}{2}$ to $7f\frac{7}{2}$, using separable quadrupole particle-hole forces with an unlike-to-like nucleon-nucleon interaction ratio $\beta/\alpha = 3$. For ^{118}Sn we needed $\alpha = -9.6 \times 10^{-4}$ MeV fm^{-4}, to place the 2_1^+ state at the empirical energy. An effective mass ratio of 0.75 was necessary to place the GQR at about $64A^{-1/3}$ and to obtain a realistic amount of core polarization in the low-lying 2^+ state from the giant resonances. All significant giant-resonance strength in the range 8 to 16 MeV lies in five excitations from 9.5 to 13.2 MeV, dominated by one state at 13.2 MeV with $M_n/M_p = 60.3/53.9 = 1.12$. Defining M_n/M_p as the rms sums over these five states, we get $M_n/M_p = 1.14$. As mentioned in Sec. III, this is somewhat lower than the (degenerate) schematic model quoted above for the same value of r_n/r_p. The two calculations are different in that, for equal average two-quasiparticle energies, the interaction must be much greater in the degenerate case to push the isoscalar GQR down to the empirical value of $64A^{-1/3}$. These results are summarized in Table II as set A. For comparison, we

TABLE II. Neutron and proton multipole matrix elements M_n and M_p in fm^2 calculated from a nondegenerate RPA code using a separable interaction and including pairing. The calculation is described in Sec. IV. M_n and M_p are given for the isoscalar giant-quadrupole resonance (GQR) and the 2_1^+ transition in ^{118}Sn. Case A uses a realistic neutron skin of $r_n/r_p=1.04$; Case B uses $r_n/r_p=1.1$.

	GQR (13.2 MeV)			2_1^+ (1.23 MeV)		
Case	M_n	M_p	M_n/M_p	M_n	M_p	M_n/M_p
A	60.3	53.9	1.12	72.8	42.5	1.71
B	73.6	44.1	1.67	91.1	43.2	2.11

Empirical (GQR): $M_p=63.0\pm13.0$[a] and $M_n/M_p=1.9\pm0.4$ with $M_p=31.0\pm1.3$[b]
Empirical (2_1^+): $M_p=45.5\pm0.4$[c] and $M_n/M_p=1.72\pm0.21$[d]
$=1.27\pm0.26$[e]

[a]Based on sum-rule estimate for ^{116}Sn from Ref. 13 (arbitrary 20% error).
[b]See Ref. 7 and footnote b of Table I.
[c]$M_p=[B(E2)\uparrow]^{1/2}$ from Ref. 2.
[d]See Refs. 2 and 14.
[e]See footnote e of Table I.

also performed the same calculation with $r_n/r_p=1.10$, which gives the results labeled set B. This unreasonably large neutron skin is used to more nearly obtain the pion GQR results for M_n/M_p. The expectation was that the M_n/M_p resulting from this unphysical neutron skin would be unacceptably different from the existing data[2,7] on the low-lying transition.

In the results presented so far we have only considered the multipole matrix elements. These are the λth moments of the mass transition densities[16] which may be seen explicitly by rewriting Eq. (1) in the form

$$M_{(n,p)}=\int \rho^m_{\lambda(n,p)}(r)r^{\lambda+2}dr \ , \tag{8}$$

with the transition densities defined by[16,17]

$$\rho^m_{\lambda(n,p)}(r)=\left\langle f \left| \left| \sum_{i=i}^{(N,Z)} \frac{\delta(r-r_i)}{r_i^2} Y_\lambda(\hat{\mathbf{r}}_i) \right| \right| i \right\rangle . \tag{9}$$

It is the transition densities that contain the complete model information concerning the transition. The multipole matrix elements, which are uniquely determined only via electromagnetic data at the photon point, clearly measure the transition densities in the tail region.

Inelastic scattering cross sections depend, in general, on somewhat different features of the transition densities, and these reactions can, in some cases, provide detailed information on the radial profile of the densities.[16,18] For example, pions at 130 MeV are strongly absorbed so the cross sections at the first peak are sensitive to the densities just beyond the nuclear surface and are expected to follow the multipole matrix elements. Low energy nucleons experience moderate absorption and refraction, so they are also sensitive to the surface properties of the densities. These reactions are the ones being considered here. Electrons and intermediate energy nucleons are, on the other hand, sensitive to interior details of the transition densities.

The experimental values of M_n and M_p obtained from hadronic data, that have been discussed above, have been extracted using certain models. In particular, the nucleon scattering values are based on the collective model for inelastic nucleon scattering described in Ref. 1 and the pion scattering values are based on cross section formulas obtained from the idea of Δ dominance for pion-nucleus scattering.[19] Here we examine the transition densities predicted by our quasiparticle RPA model. In the next section we use these densities in fully microscopic calculations of inelastic scattering observables. These calculations provide a good indication of the consistency between the model assumption used in extracting M_n and M_p above and the current microscopic models for calculating inelastic cross sections.

The relevant transition densities are shown in Fig. 1 as a function of radial position. They are based on harmonic-oscillator radial wave functions. For the GQR

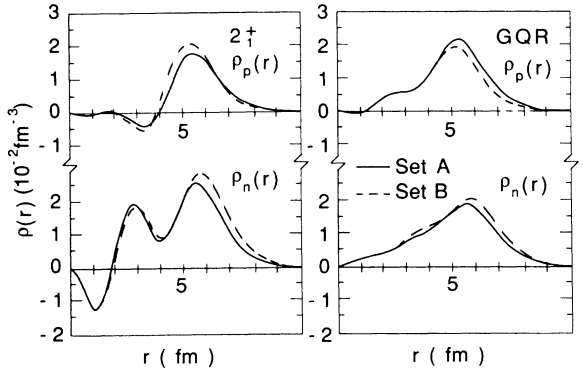

FIG. 1. The proton (top) and neutron (bottom) matter transition densities for the first ($E_x=1.23$ MeV) 2^+ state (left) and the dominant $E_x=13.2$ MeV state in the GQR region (right) of ^{118}Sn. The solid curve is the result of our standard calculation, set A, while the dashed curve results when a larger neutron radius is employed in set B.

we show only the dominant contribution from the 13.2 MeV level. The solid curve denotes set A ($r_n/r_p=1.04$) while the dashed curve denotes set B ($r_n/r_p=1.10$). Of particular note is the difference between ρ_n and ρ_p for the 2_1^+ transition. We also see that the neutron densities stick our farther than the proton densities and have longer tails. The radial difference is about 0.2 fm for set A and somewhat more for set B. To be more complete it would be necessary to include Coulomb effects in a Woods-Saxon basis and consider the unbound nature of the GQR. Preliminary results for ^{208}Pb indicate that the use of more realistic radial wave functions does not produce large effects in the transition densities.[20]

V. SCATTERING CALCULATIONS

In this section we present the results of parameter-free folding model calculations for inelastic electron, nucleon, and pion scattering which use the RPA transition densities described in Sec. IV as the common nuclear structure input. For the first 2^+ transition we consider the available electromagnetic data along with cross section data from low energy proton[21] and neutron[22] scattering and the 130 MeV pion work of Ref. 7. The low energy nucleon data are the same as those used in extracting M_n/M_p in Ref. 2. For the GQR we consider the pion cross section data of Ref. 7, and, in the absence of electromagnetic data for ^{118}Sn, the electron cross section data of Ref. 13 for ^{116}Sn. The value of M_p for the GQR in ^{116}Sn is expected to be similar to that for ^{118}Sn.

The reaction model used in the present calculations can be neatly summarized by presenting the relevant terms from the general plane-wave Born cross-section formula for natural parity transitions excited by electrons, nucleons, and pions.[16] In this case, where only the matter transition densities were produced by the RPA code (under the reasonable assumption that these dominate the scattering process for collective excitations such as the 2_1^+ and the GQR), the $0^+\rightarrow\lambda^\pi$ [$\Delta\pi=(-1)^\lambda$] Born cross section contains only two terms

$$\frac{d\sigma}{d\Omega}=4\pi\left[\frac{\mu}{2\pi\hbar^2}\right]^2[\,|\,t^{C0}\rho_\lambda^m\,|^2+f(\theta)\,|\,t^{LS}\rho_\lambda^m\,|^2]\,, \qquad (10)$$

where t^{C0} is the spin independent central coupling (for electrons, nucleons, or pions), t^{LS} is the spin-orbit coupling (for nucleons only), ρ_λ^m is the matter (particle number) transition density; there is an implied coherent sum on the proton and neutron components of the $t\rho$ products, and $f(\theta)$ is an angle-dependent factor from the plane-wave matrix element of a current operator. Antisymmetrization for the nucleon scattering calculations is treated in a short range approximation which neglects convection current contributions for these transitions.[23] For electromagnetic observables it is more convenient to refer to

$$B(E\lambda;q)=|\,\rho_{\lambda,p}^m(q)\,|^2 \qquad (11)$$

instead of $d\sigma/d\Omega$. Note that Eqs. (9) and (11) lack a $(2\lambda+1)$ factor relative to the definition in Ref. 16 (see Ref. 17). Note also that $B(E2)\uparrow$ in Tables I–III is equal to $B(E2;0)=M_p^2$ in e^2fm^4 with these conventions.

The actual scattering calculations for the hadronic probes must include the effects of the mean nuclear field. This is done in the distorted wave approximation (DWA). The specific procedure is to generate a transition potential in ALLWRLD (Ref. 24) from the RPA matter transition densities and appropriate effective interactions t^{C0} and t^{LS}. These are read into a DWA code [TAMURA (Ref. 25) for nucleons, MSUDWPI (Ref. 26) for pions] that uses an optical potential generated self-consistently from the ground-state matter density and the same effective interaction used to obtain the transition potential.

The nucleon scattering results used von Geramb's parametrization[27] of the g matrix obtained from the HJ potential, the so-called "Brieva-Rook" set. The 24 MeV solution was used for $E_p=24.5$ MeV while the 10 MeV solution was used for $E_n=11$ MeV. These interactions require some small adjustments to reproduce elastic scattering cross sections in detail.[28] We have made no adjustments here. The pion scattering results are based on a t matrix taken from phase shifts[29] with absorption and other medium modifications included explicitly.[30] This interaction provides a reasonable description of elastic and inelastic pion scattering data in the region of interest.

Both sets of RPA transition densities are used. Set A, which came from assuming a 4% neutron skin, is consistent with the schematic model and represents the standard prediction of our model calculations. It is shown by a solid curve in the figures. We also include set B, constructed by assuming a 10% neutron skin, as an extreme case which has M_n/M_p for the GQR closer to that deduced from the pion experiments. Results for the 2_1^+ and GQR region will now be discussed separately.

A. First 2^+ state ($E_x=1.23$ MeV)

The results for 130 MeV positive and negative pion inelastic scattering to the 2_1^+ state of ^{118}Sn are shown in Fig. 2 with the experimental data.[7] The calculated and experimental differential cross sections are in fairly good agreement for negative pions but lower than the data for positive pions. The former are more sensitive to target neutrons and the latter are more sensitive to target protons. The disagreement for positive pions is puzzling, since the transition density of set A gives a value of $B(E2)=1810$ e^2fm^4, in good agreement with the experimental value[2] of $B(E2)=2070\pm60$ e^2fm^4. It would be useful to compare the charge form factor to electron scattering data, but none is available for ^{118}Sn. Using the densities of set B, which have the larger neutron radius, the π^- cross section increases along with the neutron strength, becoming somewhat higher than the data. There is also a small increase in the proton strength, giving $B(E2)=1866$ e^2fm^4 for set B. This is presumably due to increased polarization of $2\hbar\omega$ proton transitions by the valence neutrons, which have a larger radius in set B, even though the protons will have a decreased strength due to their smaller radius. The experimental value of $M_n/M_p=1.27\pm0.26$,[7] compared to the value of

1.72 ± 0.21 from other probes[2,14] reflects the large values of the π^+ data in Fig. 2. The cross section ratio $R(\theta)=\sigma_{\pi^-}(\theta)/\sigma_{\pi^+}(\theta)$ is plotted in the bottom third of the figure. The rapid angular dependence of this ratio, due to the relative shift of the π^+ and π^- diffraction minima, shows the prudence of the comparison of full angular distributions with DWA calculations (rather than simple force-ratio arguments based on cross sections at a particular angle) in the extraction of M_n/M_p ratios. We think it is more important to emphasize the failure to fit $\sigma_{\pi^+}(\theta)$ than the failure to fit $R(\theta)$.

The calculated nucleon inelastic scattering cross sections for $E_p=24.5$ MeV and $E_n=11$ MeV are compared with data[21,22] in Fig. 3. Protons at these low energies are most sensitive to neutron densities. Set A transition densities give a reasonably good fit to the (p,p') data[21] at angles greater than about 30° and, therefore, will fit the integrated cross section fairly well, but they fall below the data at the main peak. The enhanced neutron densities of set B produce proton scattering cross sections in agreement with the data at the peak, but too high compared to data at angles greater than 30°. If we further increased r_n/r_p beyond the value used in set B to yield a ratio of $M_n/M_p=1.90$ for the GQR in agreement with the pion scattering data,[7] the resulting differential cross section would lie above even the first peak and would give much too high a total cross section. The experimental neutron inelastic cross section[22] is described fairly well by the transition densities of set A at backward angles and set B at forward angles. The transition densities of set B do not increase the neutron cross section very much relative to set A due to the fact that neutrons at this energy are rather more sensitive to nuclear protons. It has already been noted that there is only a small increase in M_p when the ratio of r_n/r_p is increased from 1.04 to 1.1.

The deficiency in the slope of the theoretical cross sections relative to the experimental data evident in Fig. 3 has been noted in earlier microscopic calculations for low-energy nucleon-nucleus scattering which use empirically determined densities.[31] This is a real deficiency in the model which is presumably associated with exchange and rearrangement corrections to the folding model. On the basis of Ref. 31, the theoretical calculations are expected to be low at forward angles. With this proviso, the nucleon scattering data are consistent with the densities of set A which have $M_n/M_p=1.71$, consistent with the results of Ref. 2.

It is very puzzling that our predicted ρ_p is consistent with the neutron scattering and electromagnetic data but

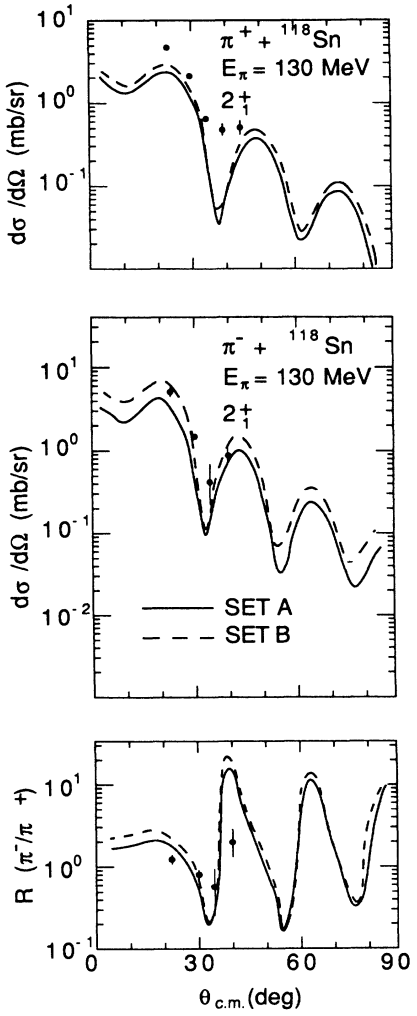

FIG. 2. Differential cross sections and π^-/π^+ cross section ratios for inelastic pion scattering to the first 2^+ state in ^{118}Sn. The solid and dashed curves are calculated from the set A and set B densities, respectively, while the 130 MeV π^+ and π^- data are from Ref. 7.

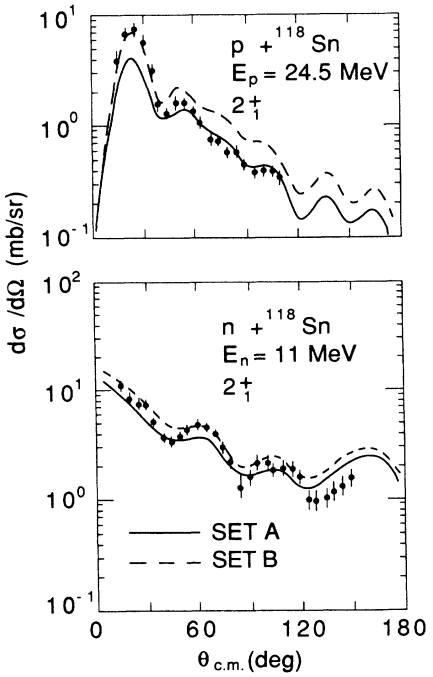

FIG. 3. Differential cross sections for inelastic nucleon scattering to the first 2^+ state in ^{118}Sn. Calculations with set A (solid curve) and set B (dashed curve) are compared to the 24.5 MeV proton scattering data of Ref. 21 and the 11 MeV neutron scattering data of Ref. 22.

fails (badly) to describe the π^+ data. In contrast, the π^- and proton calculations suggest the data are consistent with our predicted ρ_n. It is essential that we acquire good nucleon and electron scattering data at higher energies. The combination of $E_p \geq 135$ MeV and electron scattering with high resolution would allow a detailed test of the RPA densities, as would experiments at $E_n = E_p = 60$ MeV.[18] Presumably such data would also contain information regarding the reversal states,[12] which are also part of the whole picture we are examining. This is a minimal requirement for quantitative studies of the isospin structure of quadrupole excitations.

B. Giant-quadrupole-resonance region

The calculations for positive and negative pion scattering to the GQR region are compared to the data of Ullman *et al.*[7] in Fig. 4. The RPA calculations assume the GQR is made up of discrete states, so we incoherently add the cross sections for the levels in the 9 MeV $< E_x <$ 19 MeV region to obtain the angular distributions shown here. The sum is dominated by a single state near $E_x = 13.2$ MeV as noted earlier. The transition densities of sets A and B give very similar results for positive pions which are sensitive mainly to the nuclear protons. Both sets of calculated differential cross sections are much above the data. For negative pions, set A gives results fairly close to the data but a little high, while those of set B give too much cross section. This is consistent with the sensitivity of negative pions to the increase in M_n produced by the large ratio $r_n/r_p = 1.1$. These results exclude set B as having an excessively large ρ_n. We see from a comparison of the calculations of set A with the data that the large value of M_n/M_p deduced from experiment is due *not* to an unexpectedly large π^- cross section (M_n) but to an unexpectedly *small* π^+ cross section (M_p). This is opposite to the result for the 2_1^+ transition where the experimental π^+ cross section seems high. We again point out that looking only at $R(\theta)$ hides the fact that the problem is with the predicted π^+ cross section and/or the proton density. A similar conclusion has also been reached by Seestrom-Morris *et al.*[8] in a recent paper on pionic excitation of the giant resonance in ^{208}Pb.

We wish to emphasize that this question concerning the proton component of the GQR is susceptible to independent experimental tests. There exist electron scattering data for the giant resonances in ^{116}Sn from Tohoku.[13] We present these data in Fig. 5 as a band (about ±20% wide to reflect some of the experimental uncertainties) compared to our model predictions. The discrete strengths were folded with a 4 MeV Gaussian to give some spreading in comparison to data. The experimental pion data correspond to about half of the set B

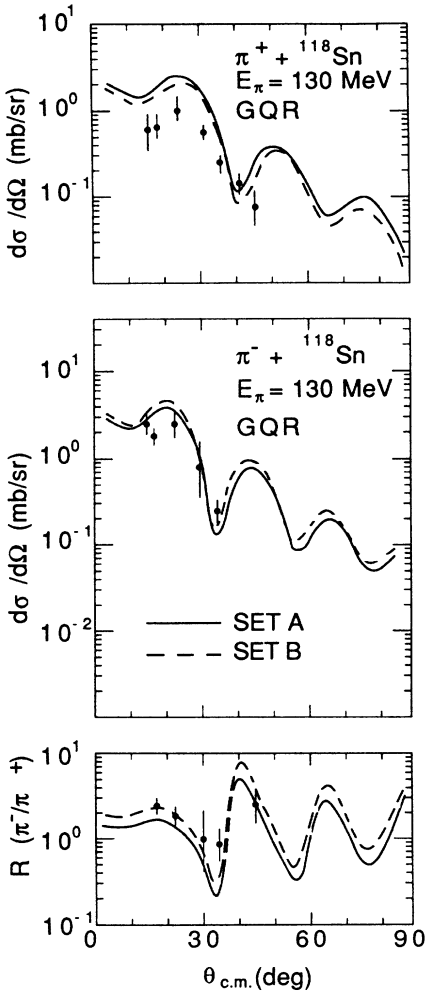

FIG. 4. Differential cross sections and π^-/π^+ cross-section ratios for excitation of the GQR in ^{118}Sn with 130 MeV pions. The data are from Ref. 7, while the solid and dashed curves were obtained using densities from set A and set B, respectively. The curves are the incoherent sums of cross sections calculated for all of the states in the GQR region.

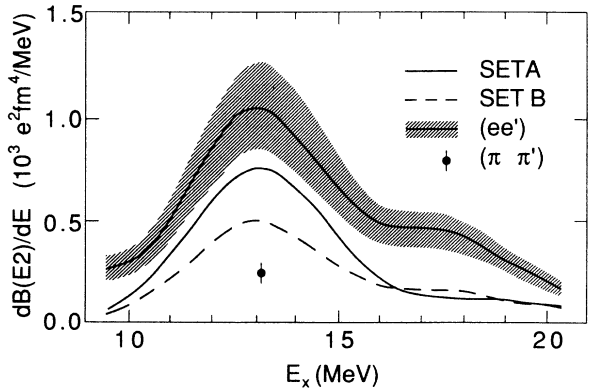

FIG. 5. Excitation function for electric quadrupole strength in ^{118}Sn. The curves are from our set A (solid curve) and set B (dashed curve) RPA calculations. The band at the top is indicative of the values obtained from the electron scattering data for ^{116}Sn in Ref. 13, while the "data" point indicates the value expected based on the M_p extracted from the pion data of Ref. 7. A Gaussian spreading width of 4 MeV was used to construct the curves (but not the "data" point) from the discrete states in our calculations and the tables of experimental data.

curve, as indicated by the "data" point in Fig. 5. Spreading effects would lower this. Although there are large systematic uncertainties in the present electron scattering data, they are most consistent with set A. The factor of 3 between set A and the pion results should be easily measurable. Ideally the results of electromagnetic measurements should be presented in a form like Fig. 5, for direct comparison to calculation, rather than in terms of derived numbers such as fraction of the $T=0$ sum rule.

The pion-scattering results, taken as a whole, indicate that it is reasonable to use the multipole matrix elements as an approximate way to summarize the data. We will do so in the remainder of this paper. There are variations of perhaps 20% or so between cross-section ratios computed from different densities with comparable M_n/M_p ratios. This is probably an indication of the size of effects attributable to the radial sensitivity of the pion, but it cannot be quantified at this time. The deficiency in our predictions of the π^+ data (about a factor of 2) are much larger than these effects.

VI. DISCUSSION

A. Comparison to other calculations

Our results of various types of calculations of the GQR all agree with each other to the extent that all lie far short of the values of M_n/M_p determined from analysis of the pion data.[7] It is of interest to compare our results with other theoretical determinations of M_n/M_p and the inelastic pion cross sections. Auerbach *et al.*[32] have done a self-consistent continuum RPA calculation with Skyrme III forces for a hypothetical closed-shell ^{120}Sn isotope. Values of the squared neutron and proton multipole matrix elements were presented and the ratios of π^+ and π^- inelastic cross sections are given at the angle corresponding to the peak in the π^- angular distribution. In our calculations this corresponds to about 20° rather than the angle of 23° where the experimental data are tabulated. Inspection of Fig. 4 indicates that for set A, $R(\theta)$ increases from the tabulated value 1.30 at 23° to 1.55 at 20° due to its rapid angular dependence. The latter value should be compared to model 3,[32] and we note that the agreement is quite good. Notice that they also predict a σ_{π^+} that is substantially above the experimental data as we do. Thus we agree on the crucial point regarding the proton content of the GQR. Because their basis is pure particle hole (not two-quasiparticle), they are unable to treat the 2_1^+ state correctly, but, as we have seen in Sec. III, this defect should not affect their results for the giant states substantially. The value of M_n/M_p for the GQR deduced from their table for the isoscalar giant resonance region is 1.45, which is close to the value of $N/Z=1.40$ but somewhat greater than any of our results except that obtained with an unrealistic ratio of neutron to proton rms radii. They do not report on the ground-state densities from the Hartree-Fock calculation used as a basis for the particle-hole states in the RPA calculation, but one of the authors[33] has assured us that the neutron and proton densities have reasonable rms radii.

We expect that all calculations of the giant-resonance strengths would tend to reduce the ratio of M_n/M_p from the unperturbed values due to the interaction between the neutrons and protons. On that basis one might then wonder why this ratio is equal to N/Z in Ref. 32. The explanation is likely that the continuum calculations favor neutrons compared to protons in the particle component of the particle-hole states. This effect could compensate for the reduction of M_p relative to M_n by the interaction, giving a result closer to the hydrodynamical value of N/Z. This possibility can be examined by comparing calculations of neutron to proton excitations for the isoscalar giant resonance in ^{208}Pb. The continuum effects should be less important for this nucleus because the particle-hole excitations are lower in energy and should put the particle lower in the continuum, where neutron and proton wave functions are more nearly equal. Indeed, Ref. 32 gives a relatively lower ratio in ^{208}Pb ($M_n/M_p=1.42$ compared to $N/Z=1.57$) than in ^{120}Sn with ($M_n/M_p=1.45$ compared to $N/Z=1.40$). Our calculations in ^{208}Pb give $M_n/M_p=1.50$, which is much closer to Ref. 32 than are our ^{118}Sn results. In the Jülich calculation[34] often used in comparing to data, the ratio is N/Z for ^{208}Pb. The RPA results of Ref. 34 include a discretized continuum but no two-particle two-hole effects. From these considerations one cannot conclude that the ^{120}Sn results simply correspond to the continuum RPA theory being very close in physical content to the hydrodynamic model of a giant isoscalar vibration.

Another RPA calculation of the neutron and proton matrix elements for the giant isoscalar excitation in ^{208}Pb is the one-particle one-hole plus two-particle two-hole RPA with discretized continuum states that has been done by Wambach.[35] In the one-particle one-hole calculation the ratio M_n/M_p in the region of the giant-resonance peak is ~ 1.2, but above the giant-resonance peak the ratio is much higher. When the two-particle two-hole components are included in the RPA, the ratio in the isoscalar giant-resonance peak is very close to N/Z. Perhaps as the quantum calculation basis becomes enlarged to incorporate configurations beyond the simple particle-hole states, it comes closer to being capable of simulating the classical hydrodynamic model.

B. Core-polarization from the GQR as determined from π^-/π^+

As stated in a number of different ways in this paper there is an important connection between the isospin composition of the giant-quadrupole resonances and that of the low-lying 2_1^+ transitions. In order to investigate the isospin consequences on the 2_1^+ transition from the large GQR M_n/M_p deduced[7] from π^-/π^+, we use the RPA schematic model of core polarization but constrain M_n/M_p to be 1.9 for the isoscalar GQR. The core-polarization effects are calculated using Eqs. (5). The input parameters are the same as used in the four-state diagonalization described in Sec. III. The results for M_n and M_p for the GQR and the 2_1^+ transition are shown in Table III. Case a shows the results with standard input parameters. The fact that M_n and M_p for the 2_1^+ transi-

tion are slightly weaker in Table III than in Table I is due to the fact that perturbation theory is used for the core-polarization calculation, instead of the exact diagonalization used in the four-state problem. In particular, the effect of the reversal state, which is closer in energy to the 2_1^+ state than are the giant resonances, is somewhat stronger in the four-state diagonalization than in perturbation theory. Nevertheless, the core-polarization results are quite consistent with the four-state diagonalization and, in fact, with the full nondegenerate quasiparticle RPA results shown in Table II.

For cases b, c, and d we set $M_n/M_p=1.9$ for the isoscalar GQR. For case b this is done by increasing M_n from case a. The core-polarization effect on the 2_1^+ transition is to increase M_p and M_n/M_p to values greater than the empirical ones. These incorrect core-polarization effects do not unambiguously rule out the ratio of 1.9 for the GQR, since the GQR M_p extracted from the π^+ data are smaller than that in case b. The pion GQR data are more like case c, where we reduce M_p in the GQR. For case c, the core-polarization results yield an M_p much too low for the 2_1^+ transition in contrast to the π^+ data. In addition, M_n/M_p is too large compared to the mean value[2] from previous independent probe comparisons. Furthermore, the same pion experiment[7] which gives $M_n/M_p=1.9\pm0.4$ for the isoscalar GQR gives $M_n/M_p=1.27\pm0.26$ for the 2_1^+ transition. This is in the opposite direction to what is needed from the self-consistent core-polarization isospin distribution as seen by pions.

For cases b and c, M_n/M_p is set equal to 1.9 for the isoscalar GQR with no consideration of the energy-weighted sum rule, and correspondingly no change was made in the isovector GQR. Case d has the added feature that the $2\hbar\omega$ energy-weighted sum-rule strength has been preserved for the isoscalar and isovector giant resonances. For the isovector quadrupole state M_n/M_p has changed from -1.1 to -0.75. From Table III we see that for case d the M_p is too small and M_n/M_p is too large for the 2_1^+ transition. In all cases the M_p for the isoscalar GQR is much too large compared to the M_p in Table III determined from the GQR proton sum-rule strength seen by pions.[7] We conclude from these comparisons that the pion scattering results[7] for the 2_1^+ and the GQR are inconsistent if viewed from the standpoint of an internally consistent structure model for quadrupole excitations. For testing the predictions of this model, it is crucial that the pion results be checked and cross correlated with reactions involving other probes that excite this set of states. The predicted proton transition densities should be tested with electromagnetic probes, perhaps Coulomb excitation with heavy ions[36] as well as electron scattering measurements.

C. Background subtraction

Finally, we emphasize that our results are contingent upon uncritically accepting the data and corresponding errors. It is well known that the history of giant-resonance studies contains examples of the accidental propagation of systematic background subtraction errors into the data. Bertrand[37] recommends adding a *minimum* 20% error to data when large continuum backgrounds are subtracted. In the case of the data considered here, such an uncertainty would eliminate most discrepancies between theory and experiment, since typically the missing cross section is 25–40 % of the subtracted background. It is also important to note that the background shapes assumed in the pion analyses[7,8] are very different from those used in other studies of the GQR.[36,38] A systematic understanding of the background for all probes is a necessity if the results are to be meaningfully compared. Finally, the most surprising aspect of the pion data is that the π^-/π^+ ratio for the background is as large as the ratio for the GQR, and this

TABLE III. Neutron and proton multipole matrix elements M_n and M_p in fm^2 for the isoscalar giant-quadrupole resonance (GQR) and those resulting from core polarization on the 2_1^+ transition in ^{118}Sn. The core-polarization effects are calculated using Eq. (5).

	GQR			2_1^+		
Case	M_n	M_p	M_n/M_p	M_n	M_p	M_n/M_p
a	76.7	60.3	1.27	77.5	44.6	1.73
b	114.6	60.3	1.9	102.6	48.6	2.11
c	76.7	40.4	1.9	69.2	31.0	2.23
d	89.3	46.8	1.9	78.3	38.7	2.02
Empirical		63.0±13.0[e]	1.9±0.4[f]		45.5±0.04[g]	1.72±0.21[h]
		31.0±1.3[f]				1.27±0.26[i]

[a]Quasiparticle RPA (QRPA) with standard input parameters (see text).
[b]Fix M_p (GQR) from QRPA and M_n/M_p from π^-/π^+.
[c]Fix M_n (GQR) from QRPA and M_n/M_p from π^-/π^+.
[d]Fix M_n/M_p from π^-/π^+ with GQR sum rule unchanged from case a.
[e]Based on sum-rule estimate for ^{116}Sn from Ref. 13 (arbitrary 20% error).
[f]See Ref. 7 and footnote b of Table I.
[g]$M_p=[B(E2)\uparrow]^{1/2}$ from Ref. 2.
[h]See Refs. 2 and 14.
[i]See footnote e of Table I.

background ratio would have to increase even more to get the GQR ratio we would predict. This anomaly in the excitation of *other* continuum states (if indeed that is the source of the pion background) deserves as much attention as the structure of the GQR.

VII. SUMMARY AND CONCLUSIONS

The values of M_n/M_p, which we have calculated in the quasiparticle RPA approximation, are in good agreement with experiment for the first 2^+ state. Whereas this ratio for low-lying states is highly dependent on the shell structure in a SCS nucleus like Sn, we have shown in this paper that giant resonances should not be dependent on these $0\hbar\omega$ configurations. The values of this ratio are typically less than N/Z for the isoscalar giant resonance, a result of the interactions between neutron and proton configurations. By comparison with other calculations, we conclude that the neutron multipole strength is enhanced when the particle part of a particle-hole state is properly treated in the continuum. Furthermore, the inclusion of two-particle two-hole configurations seems to raise the ratio of M_n/M_p to agree with the hydrodynamic model of a homogeneous vibration.

However, the calculations presented in this paper and those discussed in Sec. VI all differ from each other much less than they differ from the ratio of M_n/M_p which has been extracted from the analysis of pion scattering. This discrepancy does not seem to be due to effects of the difference in neutron and proton transitions in or beyond the nuclear surface, to interaction of the giant resonances with the low-lying 2^+ state, or to mixing of isovector strength into the isoscalar energy region. The key point is that M_p is "measured" to be small. Accurate medium energy nucleon and electron scattering data would provide more stringent tests of the results of these structure calculations. We emphasize that core polarization leads to an interrelationship between all quadrupole excitations in a given nucleus; experimental studies are thus of the greatest value when they provide accurate data on the full spectrum of 2^+ states.

It is perhaps fortunate that the primary disagreement between theory and data is with the π^+ scattering. Since in the region of the resonance π^+ sees mainly protons, the results can be independently tested with electron scattering. In the long-wavelength limit electron scattering can be used to map out the $B(E2)\uparrow = |M_p|^2$ as a function of excitation energy. Such a plot of the only available electron scattering data[13] for Sn was shown in Fig. 5. The comparison of calculations A and B with the pion results (represented as a "data" point in the figure) and electron scattering data would, if the electron scattering were more reliable, be quite convincing evidence that there is a problem with the π^+ scattering and not with the theory. We have included these results here to motivate the electron scattering experiments needed to help resolve this puzzle.

A report[39] on ^{208}Pb(e,e'n) has become available. In this work the giant monopole and quadrupole multipole resonances are mapped out as a function of energy using coincidence measurements and subtracting the dipole contribution by employing (γ,n) measurements. For the giant-quadrupole resonance, 62% of the energy-weighted sum rule is exhausted. This is in good agreement with the various RPA calculations described in Sec. V, and, therefore, in disagreement with the π^+ results of Ref. 8. In a separate examination[40] of M_n/M_p in ^{208}Pb(n,n') at the Crocker Lab (University of California, Davis) has been compared to (p,p')[41] in the giant-quadrupole region. The resolution is not adequate to extract the multipole contributions from the background, but the *continuum* is consistent with distorted-wave Born approximation (DWBA) ratios based on $M_n/M_p = N/Z$, unlike the pion case. The evidence is mounting that there is nothing unusual or unexpected in the isospin structure of the isoscalar giant-resonance contrary to the indication of the pion inelastic scattering results.

Two other possibilities which remain are the following. (1) There might be a problem with the extraction of the pion inelastic scattering cross sections from the data. The isoscalar resonance sits above a high background, and what is interpreted as giant-resonance excitation cross section depends on what is subtracted as background. Some theoretical calculation of the background, such as that done by Osterfeld[42] for the Gamow-Teller (p,n) resonance, would perhaps be valuable in helping to settle this question. We mention again that other experiments[36,38] use a shape for the background that is extremely different from that used for (π,π'). Certainly it is crucial for different experiments exciting the same states to deal with this problem in a consistent fashion. If there are different subtraction procedures from one probe of the giant-resonance region to another, then they should be well motivated. (2) There may be contributions in the isoscalar resonance region from transition densities or currents other than the matter density considered in this and all previous calculations. It does seem unlikely that such effects could explain the enormous ratio of M_n/M_p of 1.9 ± 0.4 for ^{118}Sn or 3.8 ± 1.2 for ^{208}Pb. These unexpectedly large deviations from isoscalar ratios remain a puzzle which needs both theoretical and experimental contributions for its solution.

ACKNOWLEDGMENTS

We would like to thank J. Ullmann for providing detailed information on the background subtraction used in their experiment. One of us (J.A.C.) would like to thank Lawrence Livermore National Laboratory for their hospitality during the preparation of this paper. The work in this paper was done in part under the auspices of the U.S. Department of Energy under Contract No. W-7405-ENG-48 at Lawrence Livermore National Laboratory and Contract No. DE-AT06-79ER-10405 at Oregon State University. It was also supported in part by the National Science Foundation and the Florida State University Supercomputer Computations Research Institute which is partially funded by the U.S. Department of Energy under Contract No. DE-FC05-85ER250000.

[1]V. A. Madsen, V. R. Brown, and J. D. Anderson, Phys. Rev. C **12**, 1205 (1975).

[2]A. M. Bernstein, V. R. Brown, and V. A. Madsen, Phys. Lett. **103B**, 255 (1981); **106B**, 259 (1981).

[3]V. A. Madsen and V. R. Brown, in *Neutron-Nucleus Collisions—A Probe of Nuclear Structure (Burr Oak State Park, Glouster, Ohio)*, Proceedings of the Conference on Neutron-Nucleus Collisions—A Probe of Nuclear Structure, AIP Conf. Proc. No. 124, edited by J. Rapaport *et al.* (AIP, New York, 1984), p. 171.

[4]V. R. Brown and V. A. Madsen, Phys. Rev. C **11**, 1298 (1975); **17**, 1943 (1978).

[5]V. A. Madsen and V. R. Brown, Phys. Rev. Lett. **52**, 176 (1984).

[6]A. Bohr and B. Mottelson, *Nuclear Structure* (Benjamin, New York, 1969), Vol. II, Chap. 6.

[7]J. L. Ullmann *et al.*, Phys. Rev. Lett. **51**, 1038 (1983); Phys. Rev. C **31**, 177 (1985).

[8]S. J. Seestrom-Morris *et al.*, Phys. Rev. C **33**, 1847 (1986).

[9]W. D. Myers and W. J. Swiatecki, Nucl. Phys. **A336**, 267 (1980).

[10]V. A. Madsen and V. R. Brown (unpublished).

[11]This is a matrix representation of Yoshida's separable RPA equations generalized to include the isovector interaction. S. Yoshida, Nucl. Phys. **38**, 380 (1962).

[12]V. R. Brown, A. M. Bernstein, and V. A. Madsen, Phys. Lett. **164B**, 217 (1985).

[13]K. Hosoyama and Y. Torizuka, Phys. Rev. Lett. **35**, 199 (1975).

[14]The mean value of $M_n/M_p = 1.72 \pm 0.21$ does not include the data of Ref. 7. It does include $M_n/M_p = 1.58 \pm 0.35$ obtained from π^-/π^+ on ^{118}Sn from W. Wharton *et al.*, LAMPF Users Newsletter **11**, 71 (1979); private communication.

[15]S. G. Nilsson, Dan. Mat. Fys. Medd. **29**, No. 16 (1955).

[16]F. Petrovich, J. A. Carr, and H. McManus, Annu. Rev. Nucl. Part. Sci. **36**, 29 (1986).

[17]With the convention chosen for reduced matrix elements in this paper and Refs. 1–5 and 12, ρ_λ^n defined here is $(2\lambda+1)^{1/2}$ larger than that defined in Ref. 16.

[18]J. A. Carr, F. Petrovich, and J. J. Kelly, in *Neutron-Nucleus Collisions—A Probe of Nuclear Structure (Burr Oak State Park, Glouster, Ohio)*, Proceedings of the Conference on Neutron-Nucleus Collisions—A Probe of Nuclear Structure, AIP Conf. Proc. No. 124, edited by J. Rapaport *et al.* (AIP, New York, 1984), p. 230.

[19]We have in mind expressions like $\sigma_{\pi^-}/\sigma_{\pi^+} = |(3M_n + M_p)/(M_n + 3M_p)|^2$, which are commonly used in Refs. 2, 3, 5, 7, and 8 above.

[20]A preliminary calculation for ^{208}Pb to compare to the π^-/π^+ data of Ref. 8 indicates that the results for M_n and M_p for the GQR and the 2_1^+ transition with a Saxon-Woods basis are very close to those obtained using a harmonic-oscillator basis. The radial shapes of the transition densities may differ somewhat more.

[21]O. Beer *et al.*, Nucl. Phys. **A147**, 326 (1970).

[22]R. W. Finlay *et al.*, Nucl. Phys. **A338**, 45 (1980).

[23]F. Petrovich, H. McManus, V. A. Madsen, and J. Atkinson, Phys. Rev. Lett. **22**, 895 (1969); F. Petrovich, J. A. Carr, J. Philpott, and A. W. Carpenter, submitted to Phys. Rev. Lett.; see also Bull. Am. Phys. Soc. **30**, 1269 (1985).

[24]J. A. Carr, F. Petrovich, D. Halderson, and J. Kelly, computer code ALLWRLD (unpublished).

[25]J. Kelly, D. Halderson, and J. A. Carr, computer code TAMURA (unpublished) consisting of major modifications of a code similar to VENUS by T. Tamura, W. R. Cocker, and F. Rybicki, Comput. Phys. Commun. **2**, 94 (1971).

[26]J. A. Carr, computer code MSUDWPI (unpublished), adapted from the code DWPI, R. A. Eisenstein and G. A. Miller, Comput. Phys. Commun. **11**, 95 (1976).

[27]F. A. Brieva and J. R. Rook, Nucl. Phys. **A291**, 299 (1977); **A297**, 206 (1978); **A307**, 493 (1978); the numerical values were provided by H. von Geramb, private communication.

[28]The deep real potential is given to a few percent, but there can be 30% errors in the weak imaginary potential. See F. S. Dietrich *et al.*, Phys. Rev. Lett. **51**, 1629 (1983); S. Mellema *et al.*, Phys. Rev. C **28**, 2267 (1983); S. Mellema *et al.*, *ibid.* **36**, 577 (1987) for examples in $A = 208$, 56, and 89. The indirect effects of these deficiencies on a DWA calculation are much less than are seen in elastic scattering itself.

[29]G. Rowe, M. Salomon, and R. M. Landau, Phys. Rev. C **18**, 584 (1978).

[30]J. A. Carr, Ph.D. thesis, Michigan State University (unpublished).

[31]F. S. Dietrich and F. Petrovich, see Ref. 18, p. 90.

[32]N. Auerbach, A. Klein, and E. R. Siciliano, Phys. Rev. C **31**, 682 (1985).

[33]N. Auerbach, private communication.

[34]J. Wambach *et al.*, Nucl. Phys. **A324**, 77 (1979).

[35]J. Wambach, Phys. Rev. C **31**, 1950 (1985).

[36]D. J. Horen, J. R. Beene, and F. E. Bertrand, Phys. Rev. C **37**, 888 (1988).

[37]F. E. Bertrand, Annu. Rev. Nucl. Sci. **26**, 457 (1976), see Sec. 3.2.

[38]D. K. McDaniels *et al.*, Phys. Rev. C **33**, 1943 (1986); Phys. Lett. **162B**, 277 (1985).

[39]G. O. Bolme *et al.*, Phys. Rev. Lett. (unpublished); C. N. Papanicolas (private communication).

[40]E. L. Hjort *et al.*, Bull. Am. Phys. Soc. **32**, 1572 (1987); (unpublished).

[41]F. E. Bertrand and D. C. Kocker, Phys. Rev. C **13**, 2241 (1973).

[42]F. Osterfeld, Phys. Rev. C **26**, 762 (1982); later papers are reviewed by D. Cha and F. Osterfeld, in *Anti-nucleon and Nucleon-Nucleus Interactions*, edited by G. E. Walker *et al.* (Plenum, New York, 1985).